J Mol Biol. Author manuscript; available in PMC 2015 July 07.

Published in final edited form as:
J Mol Biol. 2008 April 25; 378(2): 337–352. doi:10.1016/j.jmb.2008.02.056.

Peptide-Based Interactions with Calnexin Target Misassembled Membrane Proteins into Endoplasmic Reticulum-Derived Multilamellar Bodies

Vladimir M. Korkhov[1,2], **Laura Milan-Lobo**[1], **Benoît Zuber**[2], **Hesso Farhan**[1], **Johannes A. Schmid**[3], **Michael Freissmuth**[1,*], and **Harald H. Sitte**[1]

[1]Institute of Pharmacology, Center of Biomolecular Medicine and Pharmacology, Medical University Vienna, Waehringer Strasse 13a, A-1090 Vienna, Austria

[2]Institute of Vascular Biology, Center of Biomolecular Medicine and Pharmacology, Medical University Vienna, Waehringer Strasse 13a, A-1090 Vienna, Austria

[3]MRC Laboratory of Molecular Biology, Cambridge CB2 2QH, UK

Abstract

Oligomeric assembly of neurotransmitter transporters is a prerequisite for their export from the endoplasmic reticulum (ER) and their subsequent delivery to the neuronal synapse. We previously identified mutations, e.g., in the γ-aminobutyric acid (GABA) transporter-1 (GAT1), which disrupted assembly and caused retention of the transporter in the ER. Using one representative mutant, GAT1-E101D, we showed here that ER retention was due to association of the transporter with the ER chaperone calnexin: interaction with calnexin led to accumulation of GAT1 in concentric bodies corresponding to previously described multilamellar ER-derived structures. The transmembrane domain of calnexin was necessary and sufficient to direct the protein into these concentric bodies. Both yellow fluorescent protein-tagged versions of wild-type GAT1 and of the GAT1-E101D mutant remained in disperse (i.e., non-aggregated) form in these concentric bodies, because fluorescence recovered rapidly ($t_{1/2}$ ~500 ms) upon photobleaching. Fluorescence energy resonance transfer microscopy was employed to visualize a tight interaction of GAT1-E101D with calnexin. Recognition by calnexin occurred largely in a glycan-independent manner and, at least in part, at the level of the transmembrane domain. Our findings are consistent with a model in which the transmembrane segment of calnexin participates in chaperoning the inter- and intramolecular arrangement of hydrophobic segment in oligomeric proteins.

Keywords

calnexin; neurotransmitter transporters; GABA transporter-1; G protein-coupled receptors; transmembrane domains

[*]*Corresponding author*.michael.freissmuth@meduniwien.ac.at.

Europe PMC Funders Author Manuscripts

Introduction

Neurotransmitters are released into the synaptic cleft from the presynaptic specialization and their action at pre- and postsynaptic receptors is limited in most instances by rapid re-uptake via specific transporters. Neurotransmitter transporters are thus responsible for rapid inactivation of the signals evoked at the postsynaptic neuronal membrane by their cognate neurotransmitters. Prominent among the protein families involved in this process is the neurotransmitter:sodium symporter (NSS) family, which includes carriers for serotonin (SERT), dopamine (DAT), norepinephrine, glycine, γ-amino butyric acid [GABA transporter (GAT)1–4] and a range of amino-acid and orphan transporters.[1] The mammalian members of the NSS family have been extensively studied.[2] They are predicted to possess 12 transmembrane segments and to share the same topology and several additional structural features based on the sequence similarity among various NSS members. The structure of a homologous bacterial protein, leucine transporter LeuT, has recently been solved by X-ray crystallography[3] and thus serves as a template to explore the structural basis of the translocation process.[4]

Biogenesis of membrane proteins relies on the following initial reactions: (i) the first hydrophobic peptide segment emerges from the ribosome and is (ii) recognized by the signal recognition particle, which mediates translation arrest and (iii) targeting to the translocon complex (Sec61) for insertion of the hydrophobic segment into the endoplasmic reticulum (ER) membrane. Translation resumes and, hence, membrane insertion of the remaining hydrophobic segments is concomitant with protein synthesis. Folding and possible oligomeric assembly occurs in the ER (for detailed overview, see Refs. [5,6]). Membrane proteins are hydrophobic and hence prone to aggregation. To prevent protein aggregation and to direct the folding pathway to a “native” conformation, the newly synthesized proteins appearing in the ER membrane are immediately bound by the ER resident chaperones—BiP, calreticulin, PDI, etc.[7] Interactions of ER chaperones with luminal substrate proteins have been extensively characterized. However, for membrane proteins, information is limited. Chaperones that assist folding of soluble proteins are unlikely to suffice because they cannot prevent aggregation of the membrane-embedded protein segments. In many instances, the membrane-embedded portion represents the bulk of the transmembrane (TM) protein.

The number of identified chaperones for membrane proteins is very limited. The subunits of the translocon complex (SecYEG in prokaryotes, Sec61 in eukaryotic organisms) help membrane proteins to assemble.[8] Similarly, a bacterial YidC, which mediates Sec-independent protein insertion into the membrane, assists transmembrane domain folding.[9] A membrane protein chaperone, Shr3p, has been identified in yeast.[10,11] Calnexin is an ER resident membrane-associated chaperone with a type I membrane topology: it has an N-terminal luminal lectin domain, a transmembrane domain and a cytosolic C-terminus rich in acidic residues. The sequence of calnexin is conserved in vertebrates,[12] and related proteins have been identified in all eukaryotes, including yeast.[13] The fundamental function of calnexin is to bind the carbohydrate moieties attached to the newly synthesized proteins in the ER and to assist the folding of the bound proteins.[14,15] In addition to assisting protein folding, calnexin participates in protein degradation by passing the non-refoldable substrates to ER degradation enhancing mannosidase-like protein.[16] Several studies reported the

glycan-independent interactions of calnexin with its substrates, including interactions mediated by its TM region.[17,18] Calnexin has been implicated in several genetic diseases, including cystic fibrosis due to retention of cystic fibrosis transmembrane conductance regulator (CFTR),[19] emphysema resulting from α_1-antitrypsin deficiency[20] and hemophilia caused by misfolding of clotting factor VIII.[21] It has been shown that calnexin may segregate into specialized compartments in the ER.[22,23] Moreover, overexpression of calnexin was shown to lead to formation of multilamellar bodies that retain misfolded CFTR molecules.[24]

Our earlier work identified mutations within the second transmembrane domain of GAT1, which impaired the ability of the protein to form oligomers and to traffic to the cell surface[25]: the E101D mutant of GAT1 translocates substrate in a manner indistinguishable from that of the wild-type transporter and is thus likely to adopt a native conformation. Nevertheless, GAT1-E101D is not efficiently exported from the ER because it fails to assemble correctly. The available biochemical or structural data cannot explain why the oligomerization and ER export of the mutant GAT1 fail. Here, we show that calnexin actively participates in the retention of the misassembled GAT1 molecules in the ER. GAT1 and its E101D mutant are retained by interaction with calnexin in concentric bodies previously referred to as organized smooth ER (OSER) structures.[26] Furthermore, the interactions between GAT1 molecules and calnexin are only partially abolished by inhibition of glycan recognition. Recognition of the E101D GAT1 assembly defect by calnexin is peptide-based and occurs, at least in part, at the transmembrane domain level.

Results

Modulation of ER calcium and inhibition of glucosidases partially rescues misassembled GAT1 mutant at the cell surface

Membrane proteins that fail to fold correctly in the ER are known to associate with various ER resident chaperones, such as BiP, calreticulin or calnexin.[7] Treatment with agents that modulate Ca^{2+} in the ER by inhibition of the sarcoplasmic endoreticular Ca^{2+} ATPase in some instances rescued the misfolded ΔF508-CFTR mutants and allowed for its export to the cell surface.[27,28] We tested whether alteration of Ca^{2+} homeostasis in the ER afforded the rescue of cell surface targeting of the misassembled mutant GAT1-E101D. As a control, we employed the GAT1-Δ37[29]: this mutant translocates substrate in a manner indistinguishable from that of wild type. However, due to the C-terminal truncation, this mutant lacks the Sec24D-binding site ^{566}RL^{567}, which is present in the C-terminus of GAT1 and which is required for concentrative export,[30] Accordingly, like the point mutant GAT1-566RL^{567}/^{566}AS^{567}, GAT1-Δ37 only escapes from the ER in a non-concentrative manner and thus the bulk resides within the cell.[29,30] As shown in Fig. 1a, after 2 h of thapsigargin treatment, there was already some weak cell surface expression visualized using conventional epifluorescence microscopy. We quantified the effect of thapsigargin on cell surface localization of GAT1-Δ37 and GAT1-E101D by measuring cellular GABA uptake in transiently transfected cells (Fig. 1b and c, respectively): under basal conditions (unlabelled bars in Fig. 1b and c), there was very little GAT1-E101D at the cell surface; the levels of GAT1-Δ37 were substantially higher. If transfected cells were incubated at 37 °C

with 1 μM thapsigargin for 4 h, cell surface expression increased for both GAT1-E101D and GAT1-Δ37 irrespective of the fact that surface levels of the two transporters differed under control conditions. Thapsigargin causes ER stress and raises intracellular calcium. The enhanced trafficking of proteins to the plasma membrane may therefore result from a number of factors other than impaired binding of sugars by the lectin domain of calnexin and calreticulin. However, if the cells were incubated with castanospermine (bars labelled CAS; 1 mM in Fig. 1b and c), transport activity was only augmented (by about fivefold) for the GAT1-E101D mutant (Fig. 1c). Thus, cell surface expression of GAT1-E101D was subject to regulation by the glucosidase I and II inhibitor castanospermine, while that of GAT1-Δ37 was not. Wild-type GAT1 was found almost exclusively at the cell surface (Fig. 1a); accordingly, its cell surface levels and, hence, wild-type GAT1-mediated uptake were not further enhanced by exposing the cells to castanospermine or thapsigargin (data not shown).

Exogenous and endogenous calnexin forms are targeted to multilamellar OSER structures in mammalian cells

Trimming of the terminal glucose moiety by glucosidase is a prerequisite for release of folding intermediates from ER resident lectin-type chaperones. The results summarized in Fig. 1 were therefore indicative of a potential involvement of lectin chaperones, calreticulin or calnexin, in retaining the mis-assembled variant GAT1-E101D. We hypothesized that due to its transmembrane domain, calnexin was more likely to associate with the transporter. We overexpressed versions of calnexin, which were tagged on the carboxyl terminus with yellow or cyan fluorescent protein (YFP or CFP, respectively), to search for an interaction between GAT1 and calnexin. When expressed in human embryonic kidney 293 (HEK293) cells, these calnexin constructs accumulated in discrete intracellular areas (Fig. 2a) that had been previously visualized.[24] Endogenous calnexin is expressed at high levels and is therefore predicted to support concentric body formation without ectopic overexpression. This conjecture was verified by staining permeabilized HEK293 cells with an anti-calnexin antibody and by subsequently analysing these cells by immunofluorescence microscopy (Fig. 2b). We observed concentric membrane bodies, which were reminiscent of and comparable in size with the ones seen in cells overexpressing fluorescently tagged calnexin. The estimated fraction of cells containing multilamellar bodies in our HEK293 cell culture was 5–12% (out of 279 cells counted in four independent experiments). Similar structures were found in rat embryo fibroblasts (REFs; Fig. 2c), indicating that OSER structures are not an artifact present exclusively in HEK293 cells. Imaging of the anti-calnexin antibody-stained REFs in three dimensions revealed that the intracellular inclusions were not staining artifacts, which arose from membrane invaginations at cellular attachment sites, but that these structures were within the cell space (Fig. 2d).

The transmembrane domain of calnexin determines its localization in multilamellar OSER structures

Given that endogenous calnexin appeared in OSER structures, it was interesting to determine which domain(s) of calnexin accounted for this effect. A truncated form of calnexin lacking the ectodomain (TM-calnexin) was inserted into the membrane, in the absence of the signal peptide, and accumulated in the multilamellar structures in a manner

similar to that of the full-length protein, both in HEK293 cells (data not shown) and in calnexin-deficient mouse embryo fibroblasts (cnx−/− MEFs; Fig. 3a). The observation of TM-calnexin-labelled multilamellar structures in the cnx−/− cells provided evidence that the endogenous calnexin (and, by extension, its luminal domain) is not a prerequisite for induction of and targeting to multilamellar bodies.

The peptide region required for accumulation in concentric membranes was defined by several additional carboxyterminal truncations of TM-calnexin: Δ28, Δ68 and Δ82. Similarly to TM-calnexin, all were targeted to the multilamellar structures (data not shown). We substituted the TM domain of calnexin by a stretch of 10 leucine residues, which served as a membrane anchor (L_{10}-calnexin$_{cyt}$). This mutant accumulated to levels comparable to or exceeding those of wild-type calnexin or TM-calnexin (data not shown). In contrast to the constructs that contained an intact TM-domain, L_{10}-calnexin$_{cyt}$ showed a diffuse ER localization (Fig. 3b). Furthermore, co-expression of L10-calnexin-cyt with TM-calnexin or the full-length calnexin did not increase the targeting of the former to the OSER membranes (Fig. 3c, left panel). L_{10}-calnexin$_{cyt}$ was only enriched in the preformed multilamellar structures in cases of very high overexpression (not shown). In contrast, soluble C-terminal fragment of calnexin tagged with YFP was excluded from calnexin-CFP-labelled concentric membranes (Fig. 3c, right panel). This provided further support to the observation that L_{10}-calnexin$_{cyt}$ construct was ER-membrane-bound and passively partitioned into the preformed concentric membrane structures. Together, these data strongly suggest that the minimal determinants for targeting to OSER membranes are confined to the transmembrane region of calnexin.

Calnexin–calnexin interactions are enhanced in concentric bodies

In order to assess the interactions between calnexin molecules, we measured fluorescence resonance energy transfer (FRET) between CFP and YFP-tagged full-length and truncated calnexin variants in the ER and in the concentric ER membrane structures (Fig. 3d–f). The results showed that upon removal of the luminal domain of calnexin, the proximity and, therefore, protein–protein interactions between calnexin molecules increased (Fig. 3e and f). Furthermore, the interactions both of calnexin with itself and of calnexin *versus* TM-calnexin pairs were more pronounced within the OSER membranes, as determined by three-filter FRET. For comparison, the values for net resonance energy transfer (NFRET) for the negative control (CFP *versus* YFP), as well as positive cytosolic (CYFP) and integral membrane protein (C-SERT-Y) controls are shown in the inset to Fig. 3e.

The structures observed upon calnexin and TM-calnexin expression are composed of multiple stacked ER membrane layers

To confirm that the observed structures are composed of stacked ER membrane sheets, we performed cryoelectron microscopy of vitreous sections (CEMOVIS[31]). Freezing under high pressure followed by cryosectioning of the sample ensures maximal preservation of native ultrastructure of cells under investigation. Electron microscopic analysis of the sections allows for molecular-scale resolution imaging of a biological specimen, mammalian cells in our case. HEK293 cells transfected with the full-length calnexin or the truncated mutant, TM-calnexin, were subjected to this procedure (as described under Materials and Methods).

Transmission electron microscopy showed that the intracellular inclusions that we have observed were multilamellar in both cases (Fig. 4a). High-resolution images confirmed that ribosomal complexes were excluded from these structures (not shown). A detailed account of our CEMOVIS analysis of the multilamellar body ultrastructure is currently in preparation and will be described elsewhere (V.M.K. and B.Z., unpublished results).

The lectin-less variant TM-calnexin is mobile in the membrane

A simple photobleaching experiment confirmed that calnexin molecules within the concentric membrane structures were mobile and that their mobility followed the curvature of the latter. Figure 4b shows a concentric membrane body that was partially bleached in a region close to its centre. The bleaching was performed asymmetrically, initially creating a concentric membrane structure with unevenly distributed fluorescence. However, the distribution of the fluorescent material within the whorl was smoothened in a matter of seconds, clearly confirming that the structures were membranous and did not contain any significant amount of soluble fluorescent protein that would obscure fluorescence recovery after photobleaching (FRAP) observations.

Loss of the ectodomain may have rendered the resulting TM-calnexin prone to aggregation and thus enhanced resonance energy transfer. The mobility of the truncated versions of calnexin was therefore assessed in more detail by FRAP: YFP-tagged TM-calnexin was photobleached within the areas of the concentric membrane structures and fluorescence recovery was measured in these areas as shown in Fig. 4c and d. Both the full-length calnexin and TM-calnexin showed fast recovery of fluorescence upon photobleaching, with TM-calnexin displaying faster recovery kinetics (Fig. 4e). The C-terminal truncations (e.g., in TM-calnexin-Δ68) did not affect the mobility of TM-calnexin significantly (data not shown). This indicated that deletion of the lectin domain (and C-terminus) of calnexin did not impair its mobility and did not cause aggregation of the protein.

A calnexin substrate, tsVSVG, is targeted to OSER structures upon induced misfolding

The presence of an ER resident molecular chaperone, calnexin, in the concentric OSER compartments suggested that these structures might be involved in protein quality control. To test whether calnexin served the same function in the OSER compartments as in other ER subcompartments, we employed the temperature-sensitive mutant of vesicular stomatitis virus glycoprotein (tsVSVG). VSVG has a single transmembrane domain and forms homotrimers that efficiently recruit the ER export machinery and thus rapidly reach the plasma membrane. This is also true for the temperature-sensitive mutant within the permissive temperature range of 32 to 37 °C. However, a change of culture temperature to 40 °C causes trimer dissociation and misfolding of tsVSVG.[32,33] This leads to its ER retention by way of association with calnexin in a glycan- and peptide-dependent manner. We co-expressed CFP-tagged TM-calnexin with green fluorescent protein (GFP)-tagged tsVSVG in HEK293 cells co-expressing and assessed the relative distribution of the two proteins at different temperatures (Fig. 5): if the cells were kept at 37 °C, TM-calnexin and tsVSVG colocalized with TM-calnexin in 40% the observed concentric membrane bodies (Fig. 5a and b). Switching the cultures to 40 °C for 4 h resulted in strong enrichment of tsVSVG in the OSER membrane structures such that almost all of these contained the

protein (Fig. 5a and b). However, if cells were treated with 1 mM castanospermine to inhibit glucosidases and thus abrogate binding of ER resident folding intermediates to calnexin (CAS in Fig. 5a and b), there was a decline in the amount of tsVSVG targeted to TM-calnexin-stained structures (Fig. 5a). Confocal microscopy confirmed that upon castanospermine treatment in most cases there was either a complete or a partial release of tsVSVG from the TM-calnexin-stained concentric membranes (Fig. 5c). In some cases this was accompanied by either clustering of tsVSVG near, within or around the multilamellar body (Fig. 5b; tsVSVG clusters are marked with arrowheads). This experiment clearly indicated that a transmembrane substrate of calnexin (tsVSVG) was recruited to the OSER structures and that this presumably required an interaction with endogenous calnexin, which was present therein. As soon as the substrate molecules were relieved from this interaction, their attempted escape from the multilamellar bodies was observed.

GAT1 and E101D-GAT1 are targeted to the concentric membrane bodies

We co-expressed CFP-tagged wild-type GAT1 and its E101D mutant with YFP-tagged versions of calnexin and of TM-calnexin in HEK293 cells. The calnexin-stained concentric bodies were enriched with both GAT1 (Fig. 6a) and E101D molecules (Fig. 6c). Likewise, TM-calnexin colocalized with GAT1 and E101D (Fig. 6b and d). Regardless of the presence of either overexpressed calnexin or TM-calnexin, GAT1 reached the plasma membrane. In contrast, GAT1-E101D did not reach the cell surface to any appreciable extent, consistent with our previous results.[25]

Reexpression of calnexin in *cnx−/−* cells promotes entry into multilamellar bodies of GAT1 and GAT1-E101D

In concentric membranes of TM-calnexin-expressing cells, tsVSVG, a model calnexin substrate, was retained predominantly via interaction with the endogenous (full-length) calnexin: inhibition of glucosidases by castanospermine promoted release of tsVSVG from the concentric membranes (see Fig. 7). We tested whether such sugar-dependent interactions supported the colocalization of GAT1 and of GAT1-E101D with calnexin constructs in the concentric membranes by expressing the GAT1/GAT1-E101D in calnexin-negative mouse embryo fibroblasts (*cnx*−/− MEFs[34]).

Both wild-type and mutant GAT1 were expressed predominantly within the cells, with the bulk of the molecules displaying reticular staining (Fig. 7a). In the case of wild-type GAT1, low amounts of the protein were also seen at the cell surface; this is most readily evident in the extensions and membrane protrusions (Fig. 7a, left panel). [^{3}H]GABA uptake experiments confirmed poor surface expression of both proteins (Fig. 7b). GAT1 expression at the surface was about sixfold higher than that of GAT1-E101D. In the latter case, expression was at the detection limit of an uptake experiment with a radiolabelled substrate and comparable to the level seen in HEK293 cells (cf. Fig. 1c).

We transfected *cnx*−/− MEFs with calnexin and TM-calnexin; both constructs were effectively targeted to the multilamellar structures (data not shown). This proved that the entire luminal domain of calnexin is dispensable for targeting to multilamellar bodies. Co-expression of calnexin or TM-calnexin with the GAT1 or GAT1-E101D molecules did not

improve the cell surface expression (Fig. 7c and d). This was confirmed by whole-cell [^{3}H]GABA uptakes; modest increase of cell surface GAT1 and GAT1-E101D was observed, but rigorous statistical analysis (ANOVA) deemed this result insignificant. More important, in *cnx*−/− MEFs (i.e., in the absence of endogenous calnexin), both GAT1 and GAT1-E101D colocalized with the co-expressed calnexin and TM-calnexin in multilamellar bodies (Fig. 7c and d). This showed that the lectin domain of calnexin is dispensable for its interaction with GAT1 and E101D and for targeting of the transporter into the concentric membranes.

Mobility of calnexin substrates determined by FRAP

The experiments outlined above showed that calnexin molecules were not in an aggregated state in the OSER membranes and, in addition, still function as chaperones (cf. Figs. 4 and 5). Using FRAP, we verified that the fraction of wild-type GAT1 and GAT1-E101D that was trapped in the concentric bodies was also in a non-aggregated, mobile state. Co-expressed calnexin or TM-calnexin was used as a control and the experiments were performed using the regions of interest (ROIs) within the concentric membranes as in Fig. 4c–e. As evident from the data summarized in Table 1, the chaperones and their substrates were fully mobile, with $t_{1/2}$ of around 400 ms. Consistent with data shown in Fig. 4e for single transfected constructs, TM-calnexin moved at a slightly faster rate than the other proteins. These FRAP-based measurements conclusively distinguished the observed concentric structures from the aggresomes formed by some membrane protein substrates of calnexin, in particular ΔF508-CFTR. The intracellular inclusions formed by ΔF508-CFTR are essentially immobile, although the same protein is fully mobile when targeted to the concentric membranes (data not shown).

GAT1 and GAT1-E101D differ in their interaction with calnexin

To test the interactions between calnexin and the GAT1 substrates, we resorted to FRET microscopy in living HEK293 cells; resonance energy transfer was quantified by the three-filter method because this approach allowed for a quantitative comparison. In addition, the non-invasive nature of this technique minimized phototoxicity (modest levels of exposures were required for image acquisition) and the sources of artifacts arising from cell disruption and protein solubilization. Eliminating these is likely to represent a particular challenge in the study of chaperone–substrate interactions. For FRET measurements, HEK293 cells were co-transfected with plasmids driving the expression of GAT1 or GAT1-E101D and fluorescent protein-tagged calnexin or TM-calnexin and cultured for 20–24 h prior to imaging. In parallel, imaging was performed on cells, which had been pretreated with castanospermine.

In the ER, wild-type GAT1 only interacted weakly with either calnexin or TM-calnexin (Fig. 8a): NFRET was comparable in magnitude to that of the negative control (see Fig. 3e, inset, CFP *versus* YFP) and it did not differ significantly from 0. Treatment with castanospermine did not have any effect on this signal (Fig. 8a). In contrast, there was evidence for close proximity of and thus of physical interaction between GAT1 and full-length calnexin, if resonance energy transfer was assessed within the concentric bodies: NFRET values were around 0.1. If cells were pretreated with castanospermine, resonance

energy transfer was modestly but significantly reduced (Fig. 7b, upper half). Strikingly, in cells co-expressing GAT1 and TM-calnexin, there was no appreciable interaction between the two proteins regardless of whether resonance energy transfer was assessed over the ER proper or over concentric body regions (Fig. 8b, lower half). Taken together, these results clearly indicated that GAT1 was attracted into the concentric membranes in a manner that was dependent on the luminal domain of calnexin. More important, however, if glycan binding was suppressed by blockage of glucosidases with castanospermine, the fluorescence energy transfer was not completely abrogated, suggesting that there were additional peptide-based interactions between calnexin and wild-type GAT1.

In contrast to wild-type GAT1, GAT1-E101D interacted with calnexin in the diffuse regions of the ER: the net FRET between GAT1-E101D and calnexin reached values of about 0.25 (top bar in Fig. 8c). However, this interaction required the luminal domain because it was not seen with TM-calnexin (third bar in Fig. 8c). In cells pretreated with castanospermine, we observed a decrease in resonance energy transfer by about 20% (top pair of bars in Fig. 8c); as predicted, castanospermine did not affect the resonance energy transfer between TM-calnexin and GAT1-E101D (lower set of bars, Fig. 8c). If the interaction was quantified within the concentric bodies, resonance energy transfer was found to be augmented (Fig. 8d): the NFRET of the pair GAT1-E101D *versus* calnexin reached values of about 0.4, i.e., in the range observed for the intramolecular FRET with the membrane-embedded positive control, C-SERT-Y (Fig. 3e, inset). Like in the diffuse regions of the ER, the interaction of GAT1-E101D and full-length calnexin was not fully inhibited, if glycan binding by the luminal domain of calnexin was blocked by the addition of castanospermine: FRET between GAT1-E101D and full-length calnexin was only reduced by ~30% in the presence of castanospermine (Fig. 8d, upper half). However, it is worth pointing out that net FRET between GAT1-E101D and calnexin was threefold higher than that between wild-type GAT1 and calnexin (cf. top set of bars in Fig. 8b and d). This indicated that there was a stronger interaction and this was strong enough to support a stable association in the diffuse region of the ER (cf. top set of bars in Fig. 8b and d).

A similar increase in resonance energy transfer was observed between GAT1-E101D and TM-calnexin pair in the concentric bodies. The calculated NFRET reached values close to 0.1, regardless of whether or not cells had been pretreated with castanospermine (Fig. 8d, lower pair of bars). The fact that FRET was insensitive to castanospermine provided strong evidence of a direct interaction between TM-calnexin and GAT1-E101D, which is not contingent on glycan binding to endogenous calnexin that was present in the imaged areas of the concentric bodies.

Membrane proteins are selectively targeted to the concentric membranes

Recently, the dopamine receptor has been described to interact with calnexin in concentric membranes.[35] This work prompted us to test a large number of membrane proteins by co-expressing them together with fluorescent TM-calnexin to visualize concentric bodies and to thereby assess the extent of colocalization. We surmised that many proteins would be targeted to the OSER membranes. As is evident from the data summarized in Fig. 9, this was indeed the case; polytopic proteins of various families were co-localized with TM-calnexin:

(i) the ER resident proteins, GTRAP3-18 and presenilin-1,[36] were always found to be included in concentric bodies. (ii) The dopamine transporter DAT, which is related to GAT1, was observed in about half of the OSER structures visualized with fluorescent TM-calnexin. Interestingly, the serotonin transporter SERT, which is closely related to GAT1 and even more closely to the DAT, was almost always excluded from the TM-calnexin-positive concentric bodies. These differences were not accounted for by differences in expression levels because the proteins were expressed at comparable levels. The glutamate transporter EAAT3, which was tested as a proto-typical representative of the Na^+/K^+-dependent symporters, was frequently found in the concentric structures. (iii) If members of the GPCR family were tested, there was a variation comparable to that seen with transporters: for example, the A_{2A}-adenosine receptor was always found to colocalize with TM-calnexin in OSER membranes, but other receptors were only found to be occasionally colocalized with TM-calnexin (corticotropin-releasing factor receptor-2b, metabotropic glutamate receptor mGluR1 or D_2 dopamine receptor). Finally, CXCR4, the receptor for the chemokine stem-cell-derived factor-1 was only detected in these structures very rarely. (iv) Like polytopic membrane proteins, single-span proteins such as tsVSVG (Fig. 5) or ephrin-B2 (Fig. 9) were found to accumulate in OSER membranes, indicating that the presence of multiple transmembrane spans is not a prerequisite for recruitment into these concentric bodies.

Discussion

To the best of our knowledge, we demonstrate for the first time that endogenous calnexin is targeted to the multilamellar OSER membrane compartment. We consistently observed these structures regardless of whether cells were transfected or endogenous calnexin was visualized by immunostaining. Thus, these structures cannot be accounted for by experimental artifacts resulting from either the use of a fluorescently tagged protein or fixation and permeabilization, which is inherent in staining with antibodies. Various mechanisms have been previously proposed to account for the formation of OSER structures: they have been ascribed to the oligomerization properties of GFP[26] or to the luminal domain of calnexin.[24] We find these explanations incompatible with our observations in non-transfected cells stained for endogenous calnexin. In addition, according to our results, the factor critical for driving the incorporation of calnexin into OSER structures is its transmembrane segment; the luminal domain is dispensable. Conversely, neither the cytosolic portion of calnexin nor an attached GFP moiety is *per se* capable of inducing OSER structures. This conclusion is based on the observations with L10-calnexin-cyt: this membrane-anchored cytosolic portion of calnexin also comprised GFP and failed to induce multilamellar body formation and appeared to passively copopulate the concentric membranes containing calnexin or TM-calnexin. Previous reports[24,26] proposed that the multilamellar OSER structures arose as an artifact from protein overexpression. In contrast, our observations suggest that the multilamellar OSER may exist as a physiologically and pathophysiologically relevant ER-derived compartment (see below).

It has been recently appreciated that calnexin can interact with membrane-embedded substrates in a sugar-independent manner: examples include major histocompatibility complex class I molecules,[37] proteins of the myelin sheet such as the proteolipid protein

PLP[17] and the peripheral myelin protein-22 PMP22.[18] For the subunits of the skeletal muscle nicotinic acetylcholine receptor[38] and for the D_1- and D_2 dopamine receptor,[35] both glycan-dependent and polypeptide-based interactions have been documented. While these examples indicate that calnexin engages its substrates by peptide-based interactions, this concept has in the past met some resistance, because the interactions were considered to reflect artifactual association resulting from (detergent-induced) formation of protein aggregates.[39] Here we have therefore resorted to approaches that allowed for visualizing the interactions between mobile calnexin and mobile (i.e., non-aggregated) substrates in living cells. Incidentally, because we relied on FRET microscopy rather than immunoprecipitation, we could also document that calnexin preferentially formed complexes with GAT1 in the OSER. It is not clear to what extent the previously reported polypeptide-based interactions between calnexin and membrane protein substrates occurred in these structures. We suspect that for the D_2 dopamine receptor,[35] this is likely to be the case, because (i) we observed concentric bodies containing D_2 receptors and TM-calnexin (see Fig. 7). (ii) D_2 and D_1 receptor were also seen by Free *et al.* to be trapped in concentric bodies upon overexpression of calnexin.[35] (iii) Overexpression of calnexin resulted in a reduced expression of D_2 receptors.[35]

Clearly, in spite of their accumulation to high concentrations, neither GAT1 nor GAT1-E101D aggregated in the concentric bodies. This was also true for calnexin and TM-calnexin. Thus, aggregation was not the source of the increased proximity between GAT1 and calnexin in the multilamellar bodies. Our present findings and earlier observation can be rationalized by a model positing that the transmembrane portion of calnexin acts as a fence to prevent aggregation of nascent transmembrane domains and thus assists intra- and intermolecular packing of hydrophobic domains in the membrane: if the situation cannot be remedied, calnexin traps the protein in OSER structures, which reroute the protein for degradation. This hypothesis is in line with the proposal of Wanamaker and Green[38]: in their model, the transmembrane calnexin acts as a spacer to allow for ordered assembly of the nicotinic acetylcholine receptor. The individual subunits associate in a non-random fashion and incoming new subunits sequentially displace calnexin until the pentamer is correctly assembled. This model is likely to be relevant for GAT1 and possibly other related neurotransmitter transporters: GAT1 forms constitutive oligomers[40] and its ER export is contingent on oligomer formation,[41,42] presumably because efficient recruitment of COPII-coat components requires an oligomeric assembly of GAT1.[30] Accordingly, we found (i) both glycan-dependent and glycan-independent interactions of GAT1 with calnexin. (ii) In addition, and consistent with the predictions of the model, we observed that the oligomerization-deficient variant GAT1-E101D was more prone to interact tightly with both full-length and TM-calnexin than with the native protein. (iii) Mutated versions of GAT1, which lack the Sec24D binding sites, escape to the membrane by bulk flow.[30] However, this was not the case with GAT1-E101D because it was actively retained by calnexin due to its folding defect. Manipulations that interfered with the lectin-dependent binding to calnexin only caused a modest increase of GAT1-E101D at the cell surface, because the peptide-based interactions precluded its release from the ER and presumably rather targeted it to concentric membrane bodies (from where it may finally be routed to degradation). (iv) It is also worth pointing out that mutation of E101 perturbs oligomerization and hence cell

surface localization of the resulting GAT1-E101D. Thus, in our model, calnexin senses this mutated structure. In contrast, the corresponding glutamate residue in TM2 of SERT can be readily mutated without impairing ER export and cell surface localization.[43] This is supported by our data (see Fig. 9) and is consistent with the previous observation that folding of SERT is not dependent on glycan-independent interactions with calnexin.[44]

In the model outlined above, calnexin acts as spacer during oligomeric assembly until substituted by the homo- or heterooligomeric partner; the model also predicts that upon overexpression, calnexin effectively competes with oligomerization and hence with ER export and eventually targets proteins to degradation. This explains why calnexin overexpression reduces cell surface expression of active receptors.[35] It is also evident from our data that within a given family of proteins, individual representatives differ in their propensity to be redirected to concentric bodies. The difference between SERT, DAT and GAT1 was striking: these proteins are closely related, in particular DATand SERT. Similar to GAT1, the A_{2A} receptor was readily trapped in concentric bodies, while CXCR4, another G-protein-coupled receptor, rarely entered concentric membranes. The structural basis for this difference remains, at present, enigmatic. However, it is worth noting that the A_{2A} receptor is subject to stringent ER quality control.[45]

Previous observations suggested that calnexin may exist as in an oligomeric form (possibly a pentamer, based on experiments with the lumenal domain of calnexin).[46-48] The fact that we observed resonance energy transfer between calnexin molecules is consistent with the existence of oligomeric calnexin in living cells. The significance of the FRET that we observed is even greater in the case of the truncated TM-calnexin because it implies that not only the lumenal domain, but also the transmembrane and/or cytosolic part of calnexin may be involved in oligomerization. In the context of our study, the FRET experiment shows that there is a strong resonance energy transfer signal between the calnexin molecules and that it is preserved or enhanced in the absence of the lumenal domain.

In the recent past, numerous reports have noted that intracellular membrane inclusions, similar to the multilamellar structures described herein, are commonly encountered in studies involving proteins relevant to ER storage diseases. For example, a glaucoma-related protein, myocilin, is retained in the ER and colocalizes with calnexin in membranous inclusions.[49] The same is true for PMP22, a protein involved in pathogenesis of Charcot–Marie–Tooth disease and related neuropathologies, which is retained in concentric membranes.[50] Torsion dystonia is a genetic disease that is caused by mutations in the catalytic domain of the AAA-ATPase TorsinA.[51] These mutations lead to disruption of the nuclear envelope integrity and to formation of concentric membrane bodies similar to the ones we observe with calnexin. Our unpublished observations show that TorsinA mutants indeed colocalize with the calnexin within concentric bodies. It is therefore not unreasonable to assume that other calnexin substrates, such as α1-antitryspin-Z, implicated in chronic liver disease,[52] or transmembrane surfactant protein C, mutations that cause interstitial lung diseases,[53] may be retained in smooth ER-derived multilamellar structures via interactions with calnexin.

Materials and Methods

Plasmids and cDNA constructs

The cDNA encoding calnexin was isolated by PCR from a library generated from the total RNA of HEK293 cells using RT-PCR and was cloned into pEYFP vector (Clontech) using SacI/AccI restriction sites. Truncations of calnexin were generated by PCR. Rabbit anti-calnexin antibody was from Stressgen (SPA-860). Plasmid encoding GFP-tagged PS1-dn was kindly provided by Christian Haass (Munich, Germany). Plasmid encoding mGluR1-CFP was kindly provided by Laurent Fagni (Montpellier, France). Secondary anti-rabbit Cy3-labelled antibody was generously provided by Martin Werner (Vienna, Austria). Rabbit polyclonal anti-GFP antibody was from Clontech.

Cell culture and biochemical assays

HEK293 cells and cnx−/− MEF cells were grown in Dulbecco's modified Eagle's medium containing L-alanyl-L-glutamine, 10% fetal bovine serum, and 50 mg/l gentamicin or penicillin/streptomycin on 10-cm-diameter cell culture dishes at 37 °C in an atmosphere of 5% CO_2/95% air. One day before transfection, cells were replated to obtain subconfluent cultures either on glass coverslips (22 mm in diameter and placed into six-well plates, 3×10^5 cells per well plate) or on 10-cm plates (1×10^6 cells per well plate) for uptake experiments. Transient transfections were done using either the $CaPO_4$ precipitation method or Lipofectamine 2000 (Invitrogen). [^{3}H]GABA uptake experiments were performed as described previously.[25]

CEMOVIS

For CEMOVIS, cells were spun down at 1400 rpm for 5 min and resuspended in phosphate-buffered saline supplemented with 30% dextran (30% dextran–phosphate-buffered saline) (average mass, 40 kDA; Sigma-Aldrich, Buchs, Switzerland). They were introduced into the 200-mm-deep cavity of a copper membrane carrier holder (Leica, Vienna, Austria) and vitrified by high-pressure freezing with a Leica EMPACT2 apparatus. Afterwards, tubes were mounted in the tube holder of an FC6/UC6 cryo-ultramicrotome (Leica) and trimmed in pyramidal shape as previously described.[31,54] Flat specimen holders were clamped in the cryo-ultramicrotome chunk. Copper was trimmed away with a diamond knife (Diatome, Bienne, Switzerland) on part of the specimen holder and the specimen was trimmed to a pyramidal shape with the same knife. Fifty-nanometer-feed cryosections were cut with a 35° diamond knife (Diatome) under standard cutting conditions.[54] They were collected on 1000-mesh grids (Agar Scientific, Essex, UK) coated with carbon and stored in liquid nitrogen or transferred immediately to the microscope. The images were acquired with Tecnai T12 microscope under standard low-dose imaging conditions, using a TVIPS F224 (2k×2k) CCD camera.

Epifluorescence and confocal microscopy

Fluorescence microscopy was performed using a Zeiss Axiovert 200M inverted epifluorescence microscope equipped with a CoolSNAP fx cooled CCD camera (Photometrics, Roper Scientific, Tucson, AZ). The fluorescence filter sets were purchased

from Chroma (Chroma Technology Corp., Brattleboro, VT; CFP filter set: excitation 436 nm, dichroic 455 nm, emission 480 nm; YFP filter set: excitation 500 nm, dichroic 515 nm, emission 535 nm). Coverslips with attached cells were mounted in the microscope chamber and put on the microscope stage for image acquisition. Fluorescence images were acquired and analysed using the MetaMorph of MetaSeries software package (release 4.6; Universal Imaging Corp., Downingtown, PA). Confocal microscopy was performed using a Zeiss LSM510 confocal microscope. CFP and YFP images were captured in the multitrack mode using an argon laser (458- and 514-nm lines, respectively) and a 458/514-nm beam splitter. CFP was detected with a 475- to 525-nm band-pass filter and YFP with a long-pass 530-nm filter. Imaging was performed with 6% laser power and a pinhole size of 2.5 μm. For imaging of endogenous calnexin, cells were fixed with 4% paraformaldehyde, permeabilized with 0.05% Triton X-100, blocked with 3% bovine serum albumin and incubated with the anti-calnexin antibody and Cy3-labelled secondary antibody. Imaging was performed using the 544-nm laser on an LSM510 confocal microscope.

FRAP analysis

For FRAP analysis, HEK293 cells were transfected or co-transfected with plasmids encoding various CFP- and/or YFP-tagged proteins. After 24 h, the coverslips were mounted on an incubation chamber filled with Krebs–Hepes buffer (10 mM Hepes, 120 mM NaCl, 3 mM KCl, 2 mM $CaCl_2$, 2 mM $MgCl_2$, 5 mM glucose, pH adjusted to 7.5 with NaOH). Cells were examined with a 40× oil-immersion objective on a Zeiss LSM510 confocal microscope and circular ROIs were specified for bleaching and scanning (bleach regions). Time series were taken with one scan before bleaching with 100% laser power of the 458- (CFP; 50 iterations) and 514-nm lines (YFP; 20 iterations) followed by 80 scans of the bleach region (6% laser power). For maximal time resolution, the bleach regions were scanned instead of whole cells. Mean fluorescence intensities of the bleach region over time were measured using ImageJ 1.33. The normalized values were pasted into GraphPad Prism™ 3.02 for non-linear regression analysis using the equation describing a single exponential rise from a background level b to a maximum M: $y=M\text{x}(1\text{-}e^{-\text{kx}})+b$, with b being the relative fluorescence intensity immediately after the bleaching (before recovery), M representing the extent of fluorescence recovery and k defining the rate of recovery. Data were weighted by $1/y^2$ to minimize the relative distances squared (which improves the curve fitting for the initial phase of the fluorescence recovery). The half-life of fluorescence recovery $t_{1/2}$ is defined as $0.69/k$.

FRET

FRET[55] was measured with an epifluorescence microscope (Carl Zeiss TM210, Germany) using the three-filter method.[56] HEK-293 cells were seeded onto poly-D-lysine-coated glass coverslips (2.4-cm diameter; 2×10^5 cells). The next day, cells were transiently transfected using the $CaPO_4$-precipitation method. Twenty-four to 48 h after transfection, media were replaced by Krebs–Hepes buffer (10 mM Hepes, 120 mM NaCl, 3 mM KCl, 2 mM $CaCl_2$, 2 mM $MgCl_2$, 5 mM glucose, pH adjusted to 7.5 with NaOH), and images were taken using a 63× oil objective and a LUDL filter wheel that allows for rapid exchange of filters (faster than 100 ms). The system was equipped with the following fluorescence filters: CFP filter (I_{CFP}; excitation 436 nm, dichroic 455 nm, emission 480 nm), YFP filter (I_{YFP}; excitation

500 nm, dichroic 515 nm, emission 535 nm) and FRET filter (I_{FRET}: excitation=436 nm, dichroic mirror=455 nm, emission=535 nm). The acquisition of the images was performed with MetaMorph (Meta Imaging, Universal Imaging Corporation, V. 4.6.). Background fluorescence was subtracted from all images and fluorescence intensity was measured in ROIs. To calculate a normalized FRET signal (N_{FRET}), we used the following equation:

$N_{\mathrm{FRET}} = (I_{\mathrm{FRET}} - a \times I_{\mathrm{YFP}} - b \times I_{\mathrm{CFP}}) / \sqrt{I_{\mathrm{YFP}} P \times I_{\mathrm{CFP}}}$, where *a* and *b* represent the bleed-through values for YFP and CFP, respectively. Pixel-by-pixel corrected FRET (FRETc) images used in Figs. 3 and 6 were created using only the calculated dividend values from the above equation.

Acknowledgements

We thank Marion Holy for superb maintenance of cell culture. We are also grateful to Yvonne Vallis (Cambridge, UK) for providing rat embryo fibroblasts. This work was supported by Austrian Science Fund/FWF project programme grant SFB-35, Austrian National Bank grant 10507 (to H.F.) and Austrian Science Foundation grants P18072 (to H.F.), P15034 (to M.F.) and P17076 (to H.H.S.). V.M.K. is supported by a FEBS Long-term Fellowship at the MRC Laboratory of Molecular Biology.

Abbreviations

CFTR	cystic fibrosis transmembrane conductance regulator
DAT	dopamine transporter
ER	endoplasmic reticulum
FRAP	fluorescence recovery after photobleaching
FRET	fluorescence resonance energy transfer
FRETc	corrected FRET
GABA	γ-aminobutyric acid
GAT1	GABA transporter 1
GFP	green fluorescent protein
HEK293	human embryonic kidney 293
MEF	mouse embryo fibroblast
NFRET	net resonance energy transfer
NSS	neurotransmitter:sodium symporter
OSER	organized smooth ER
REF	rat embryo fibroblast
SERT	serotonin transporter
TM	transmembrane
tsVSVG	temperature-sensitive mutant of vesicular stomatitis virus glycoprotein
VSVG	vesicular stomatitis virus glycoprotein

YFP or CFP yellow or cyan fluorescent protein

References

1. Nelson N. The family of Na^+/Cl^- neurotransmitter transporters. J. Neurochem. 1998; 71:1785–1803. [PubMed: 9798903]
2. Gether U, Andersen PH, Larsson OM, Schousboe A. Neurotransmitter transporters: molecular function of important drug targets. Trends Pharmacol. Sci. 2006; 27:375–383. [PubMed: 16762425]
3. Yamashita A, Singh SK, Kawate T, Jin Y, Gouaux E. Crystal structure of a bacterial homologue of Na^+/Cl^--dependent neurotransmitter transporters. Nature. 2005; 437:215–223. [PubMed: 16041361]
4. Beuming T, Shi L, Javitch JA, Weinstein H. A comprehensive structure-based alignment of prokaryotic and eukaryotic neurotransmitter/Na^+ symporters (NSS) aids in the use of the LeuT structure to probe NSS structure and function. Mol. Pharmacol. 2006; 70:1630–1642. [PubMed: 16880288]
5. Sadlish H, Skach WR. Biogenesis of CFTR and other polytopic membrane proteins: new roles for the ribosome-translocon complex. J. Membr. Biol. 2004; 202:115–126. [PubMed: 15798900]
6. Booth PJ, High S. Polytopic membrane protein folding and assembly *in vitro* and *in vivo*. Mol. Membr. Biol. 2004; 21:163–170. [PubMed: 15204624]
7. Kleizen B, Braakman I. Protein folding and quality control in the endoplasmic reticulum. Curr. Opin. Cell. Biol. 2004; 16:343–349. [PubMed: 15261665]
8. Dalbey RE, Chen M. Sec-translocase mediated membrane protein biogenesis. Biochim. Biophys. Acta. 2004; 1694:37–53. [PubMed: 15546656]
9. Nagamori S, Smirnova IN, Kaback HR. Role of YidC in folding of polytopic membrane proteins. J. Cell Biol. 2004; 165:53–62. [PubMed: 15067017]
10. Kuehn MJ, Schekman R, Ljungdahl PO. Amino acid permeases require COPII components and the ER resident membrane protein Shr3p for packaging into transport vesicles *in vitro*. J. Cell Biol. 1996; 135:585–595. [PubMed: 8909535]
11. Kota J, Ljungdahl PO. Specialized membrane-localized chaperones prevent aggregation of polytopic proteins in the ER. J. Cell Biol. 2005; 168:79–88. [PubMed: 15623581]
12. Tjoelker LW, Seyfried CE, Eddy RL Jr. Byers MG, Shows TB, Calderon J, et al. Human, mouse, and rat calnexin cDNA cloning: identification of potential calcium binding motifs and gene localization to human chromosome 5. Biochemistry. 1994; 33:3229–3236. [PubMed: 8136357]
13. de Virgilio C, Burckert N, Neuhaus JM, Boller T, Wiemken A. CNE1, a *Saccharomyces cerevisiae* homologue of the genes encoding mammalian calnexin and calreticulin. Yeast. 1993; 9:185–188. [PubMed: 8465605]
14. Hammond C, Braakman I, Helenius A. Role of N-linked oligosaccharide recognition, glucose trimming, and calnexin in glycoprotein folding and quality control. Proc. Natl. Acad. Sci. USA. 1994; 91:913–917. [PubMed: 8302866]
15. Ellgaard L, Frickel EM. Calnexin, calreticulin, and ERp57: teammates in glycoprotein folding. Cell. Biochem. Biophys. 2003; 39:223–247. [PubMed: 14716078]
16. Molinari M, Calanca V, Galli C, Lucca P, Paganetti P. Role of EDEM in the release of misfolded glycoproteins from the calnexin cycle. Science. 2003; 299:1397–1400. [PubMed: 12610306]
17. Swanton E, High S, Woodman P. Role of calnexin in the glycan-independent quality control of proteolipid protein. EMBO J. 2003; 22:2948–2958. [PubMed: 12805210]
18. Fontanini A, Chies R, Snapp EL, Ferrarini M, Fabrizi GM, Brancolini C. Glycan-independent role of calnexin in the intracellular retention of Charcot–Marie–Tooth 1A Gas3/PMP22 mutants. J. Biol. Chem. 2005; 280:2378–2387. [PubMed: 15537650]
19. Pind S, Riordan JR, Williams DB. Participation of the endoplasmic reticulum chaperone calnexin (p88, IP90) in the biogenesis of the cystic fibrosis transmembrane conductance regulator. J. Biol. Chem. 1994; 269:12784–12788. [PubMed: 7513695]

20. Le A, Steiner JL, Ferrell GA, Shaker JC, Sifers RN. Association between calnexin and a secretion-incompetent variant of human alpha 1-antitrypsin. J. Biol. Chem. 1994; 269:7514–7519. [PubMed: 8125971]
21. Pipe SW, Morris JA, Shah J, Kaufman RJ. Differential interaction of coagulation factor VIII and factor V with protein chaperones calnexin and calreticulin. J. Biol. Chem. 1998; 273:8537–8544. [PubMed: 9525969]
22. Kamhi-Nesher S, Shenkman M, Tolchinsky S, Fromm SV, Ehrlich R, Lederkremer GZ. A novel quality control compartment derived from the endoplasmic reticulum. Mol. Biol. Cell. 2001; 12:1711–1723. [PubMed: 11408579]
23. Spiliotis ET, Pentcheva T, Edidin M. Probing for membrane domains in the endoplasmic reticulum: retention and degradation of unassembled MHC class I molecules. Mol. Biol. Cell. 2002; 13:1566–1581. [PubMed: 12006653]
24. Okiyoneda T, Harada K, Takeya M, Yamahira K, Wada I, Shuto T, et al. Delta F508 CFTR pool in the endoplasmic reticulum is increased by calnexin overexpression. Mol. Biol. Cell. 2004; 15:563–574. [PubMed: 14595111]
25. Korkhov VM, Farhan H, Freissmuth M, Sitte HH. Oligomerization of the γ-aminobutyric acid transporter-1 is driven by an interplay of polar and hydrophobic interactions in transmembrane helix II. J. Biol. Chem. 2004; 279:55728–55736. [PubMed: 15496410]
26. Snapp EL, Hegde RS, Francolini M, Lombardo F, Colombo S, Pedrazzini E, et al. Formation of stacked ER cisternae by low affinity protein interactions. J. Cell Biol. 2003; 163:257–269. [PubMed: 14581454]
27. Egan ME, Glockner-Pagel J, Ambrose C, Cahill PA, Pappoe L, Balamuth N, et al. Calcium-pump inhibitors induce functional surface expression of Delta F508-CFTR protein in cystic fibrosis epithelial cells. Nat. Med. 2002; 8:485–492. [PubMed: 11984593]
28. Norez C, Antigny F, Becq F, Vandebrouck C. Maintaining low Ca^{2+} level in the endoplasmic reticulum restores abnormal endogenous F508del-CFTR trafficking in airway epithelial cells. Traffic. 2006; 7:562–573. [PubMed: 16643279]
29. Farhan H, Korkhov VM, Paulitschke V, Dorostkar MM, Scholze P, Kudlacek O, et al. Two discontinuous segments in the carboxyl terminus are required for membrane targeting of the rat gamma-aminobutyric acid transporter-1 (GAT1). J. Biol. Chem. 2004; 279:28553–28563. [PubMed: 15073174]
30. Farhan H, Reiterer V, Korkhov VM, Schmid JA, Freissmuth M, Sitte HH. Concentrative export from the endoplasmic reticulum of the gamma-aminobutyric acid transporter 1 requires binding to SEC24D. J. Biol. Chem. 2007; 282:7679–7689. [PubMed: 17210573]
31. Zuber B, Haenni M, Ribeiro T, Minnig K, Lopes F, Moreillon P, Dubochet J. Granular layer in the periplasmic space of gram-positive bacteria and fine structures of *Enterococcus gallinarum* and *Streptococcus gordonii* septa revealed by cryo-electron microscopy of vitreous sections. J. Bacteriol. 2006; 188:6652–6660. [PubMed: 16952957]
32. Hammond C, Helenius A. Folding of VSV G protein: sequential interaction with BiP and calnexin. Science. 1994; 266:456–458. [PubMed: 7939687]
33. Mathieu ME, Grigera PR, Helenius A, Wagner RR. Folding, unfolding, and refolding of the vesicular stomatitis virus glycoprotein. Biochemistry. 1996; 35:4084–4093. [PubMed: 8672443]
34. Groenendyk J, Zuppini A, Shore G, Opas M, Bleackley RC, Michalak M. Caspase 12 in calnexin-deficient cells. Biochemistry. 2006; 45:13219–13226. [PubMed: 17073443]
35. Free RB, Hazelwood LA, Cabrera DM, Spalding HN, Namkung Y, Rankin ML, Sibley DR. D1 and D2 dopamine receptor expression is regulated by direct interaction with the chaperone protein calnexin. J. Biol. Chem. 2007; 282:21285–21300. [PubMed: 17395585]
36. Zhang J, Kang DE, Xia W, Okochi M, Mori H, Selkoe DJ, Koo EH. Subcellular distribution and turnover of presenilins in transfected cells. J. Biol. Chem. 1998; 273:12436–12442. [PubMed: 9575200]
37. Danilczyk UG, Williams DB. The lectin chaperone calnexin utilizes polypeptide-based interactions to associate with many of its substrates *in vivo*. J. Biol. Chem. 2001; 276:25532–25540. [PubMed: 11337494]

38. Wanamaker CP, Green WN. N-Linked glycosylation is required for nicotinic receptor assembly but not for subunit associations with calnexin. J. Biol. Chem. 2005; 280:33800–33810. [PubMed: 16091366]
39. Parodi AJ. Role of *N*-oligosaccharide endoplasmic reticulum processing reactions in glycoprotein folding and degradation. Biochem. J. 2000; 348:1–13. [PubMed: 10794707]
40. Schmid JA, Scholze P, Kudlacek O, Freissmuth M, Singer EA, Sitte HH. Oligomerization of the human serotonin transporter and of the rat GABA transporter 1 visualized by fluorescence resonance energy transfer microscopy in living cells. J. Biol. Chem. 2001; 276:3805–3810. [PubMed: 11071889]
41. Sitte HH, Freissmuth M. Oligomer formation by Na^+-Cl^--coupled neurotransmitter transporters. Eur. J. Pharmacol. 2003; 479:229–236. [PubMed: 14612153]
42. Farhan H, Freissmuth M, Sitte HH. Oligomerization of neurotransmitter transporters: a ticket from the endoplasmic reticulum to the plasma membrane. Handb. Exp. Pharmacol. 2006; 175:233–249. [PubMed: 16722239]
43. Korkhov VM, Holy M, Freissmuth M, Sitte HH. The conserved glutamate (Glu136) in transmembrane domain 2 of the serotonin transporter is required for the conformational switch in the transport cycle. J. Biol. Chem. 2006; 281:13439–13448. [PubMed: 16527819]
44. Tate CG, Whiteley E, Betenbaugh MJ. Molecular chaperones stimulate the functional expression of the cocaine-sensitive serotonin transporter. J. Biol. Chem. 1999; 274:17551–17558. [PubMed: 10364189]
45. Milojevic T, Reiterer V, Stefan E, Korkhov VM, Dorostkar MM, Ducza E, et al. The ubiquitin-specific protease Usp4 regulates the cell surface level of the A2A receptor. Mol. Pharmacol. 2006; 69:1083–1094. [PubMed: 16339847]
46. Ou WJ, Cameron PH, Thomas DY, Bergeron JJ. Association of folding intermediates of glycoproteins with calnexin during protein maturation. Nature. 1993; 364:771–776. [PubMed: 8102790]
47. Zapun A, Darby NJ, Tessier DC, Michalak M, Bergeron JJ, Thomas DY. Enhanced catalysis of ribonuclease B folding by the interaction of calnexin or calreticulin with ERp57. J. Biol. Chem. 1998; 273:6009–6012. [PubMed: 9497314]
48. Ihara Y, Cohen-Doyle MF, Saito Y, Williams DB. Calnexin discriminates between protein conformational states and functions as a molecular chaperone *in vitro*. Mol. Cell. 1999; 4:331–341. [PubMed: 10518214]
49. Liu Y, Vollrath D. Reversal of mutant myocilin non-secretion and cell killing: implications for glaucoma. Hum. Mol. Genet. 2004; 13:1193–1204. [PubMed: 15069026]
50. Fortun J, Li J, Go J, Fenstermaker A, Fletcher BS, Notterpek L. Impaired proteasome activity and accumulation of ubiquitinated substrates in a hereditary neuropathy model. J. Neurochem. 2005; 92:1531–1541. [PubMed: 15748170]
51. Walker RH, Shashidharan P. Developments in the molecular biology of DYT1 dystonia. Mov. Disord. 2003; 18:1102–1107. [PubMed: 14534912]
52. Kamimoto T, Shoji S, Hidvegi T, Mizushima N, Umebayashi K, Perlmutter DH, Yoshimori T. Intracellular inclusions containing mutant alpha1-antitrypsin Z are propagated in the absence of autophagic activity. J. Biol. Chem. 2006; 281:4467–4476. [PubMed: 16365039]
53. Mulugeta S, Nguyen V, Russo SJ, Muniswamy M, Beers MF. A surfactant protein C precursor protein BRICHOS domain mutation causes endoplasmic reticulum stress, proteasome dysfunction, and caspase 3 activation. Am. J. Respir. Cell. Mol. Biol. 2005; 32:521–530. [PubMed: 15778495]
54. Studer D, Graber W, Al-Amoudi A, Eggli P. A new approach for cryofixation by high-pressure freezing. J. Microsc. 2001; 203:285–294. [PubMed: 11555146]
55. Schmid JA, Sitte HH. Fluorescence resonance energy transfer in the study of cancer pathways. Curr. Opin. Oncol. 2003; 15:55–64. [PubMed: 12490762]
56. Xia Z, Liu Y. Reliable and global measurement of fluorescence resonance energy transfer using fluorescence microscopes. Biophys. J. 2001; 81:2395–2402. [PubMed: 11566809]

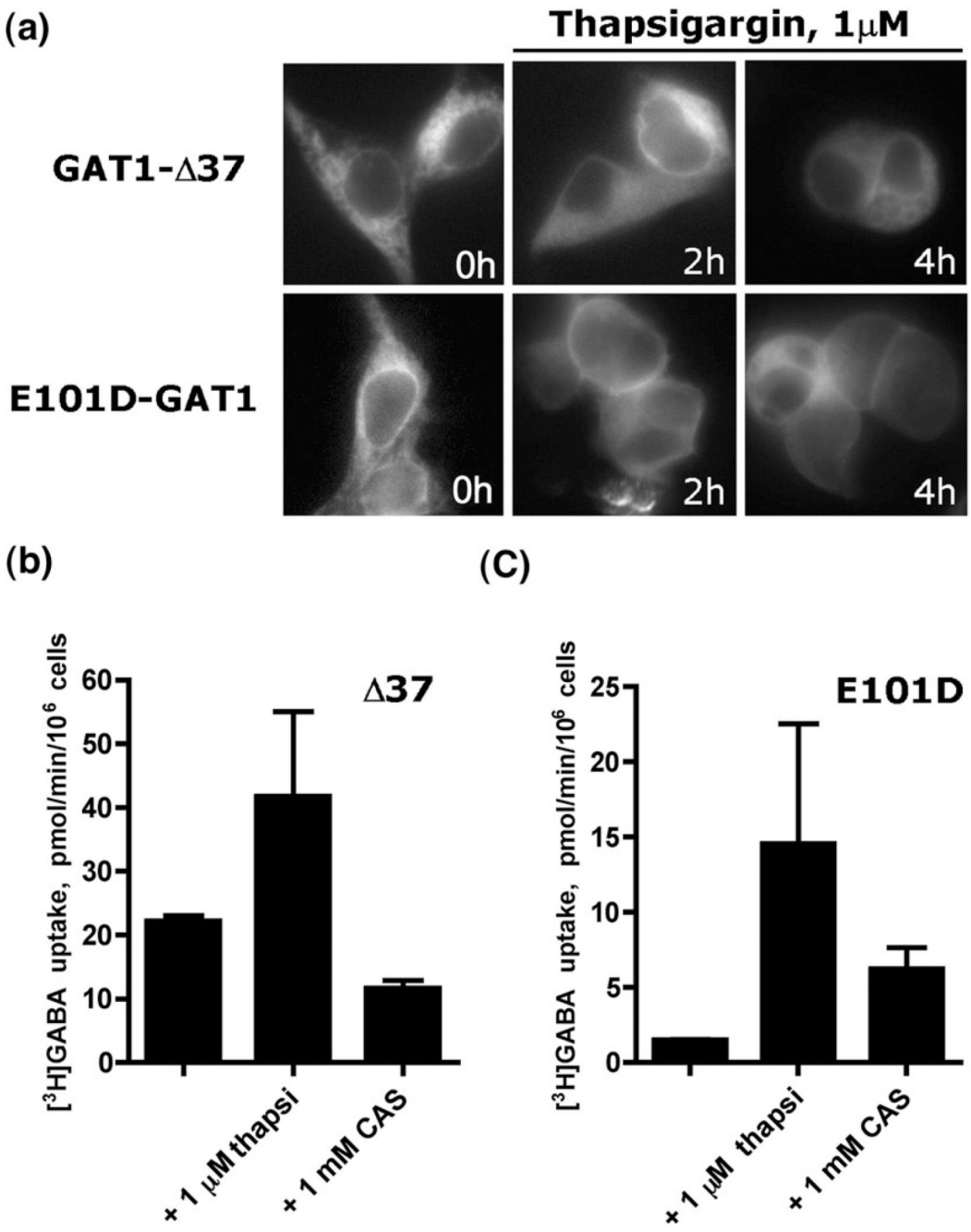

Fig. 1.

Depletion of calcium from ER or inhibition of ER glucosidases rescues cell surface expression of GAT1-E101D mutant. (a) Fluorescence microscopy of HEK293 cells transfected with GAT1-Δ37 or GAT1-E101D and treated with 1 μM thapsigargin. Cell surface expression of GAT1-E101D is evident after 4 h. (b) Whole-cell [^{3}H]GABA uptake by GAT1-Δ37 or GAT1-E101D (c) following treatment with 1 μM thapsigargin (thapsi) or 1 mM castanospermine (CAS). The data shown are means of two independent experiments; error bars indicate SD.

Europe PMC Funders Author Manuscripts

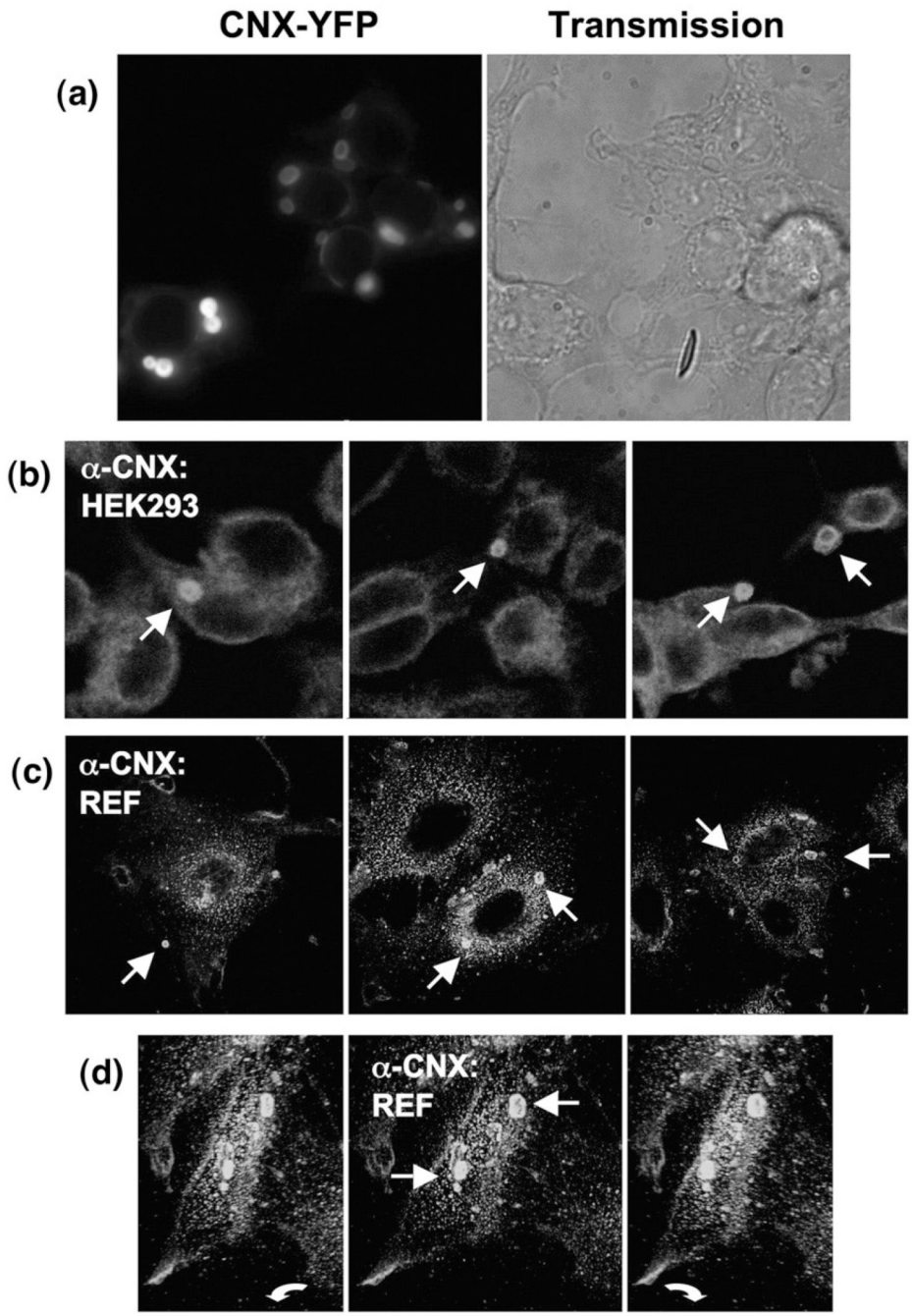

Fig. 2.

Endogenous calnexin is targeted to the concentric bodies (corresponding to OSER) in mammalian cells. (a) Fluorescence microscopy reveals concentric membrane formation by a YFP-tagged full-length calnexin in transfected HEK293 cells. (b) Immunofluorescence microscopy of HEK293 cells stained with an antibody directed against the last carboxyterminal residues of calnexin (anti-rabbit secondary antibody labelled with Cy3). (c) Same as in (b), but performed using REFs. (d) A z-stack of a REF cell stained for

endogenous calnexin was rendered in 3-D; three views of the resulting model are shown under an angle of ~30°; arrows indicate the OSER structures.

Europe PMC Funders Author Manuscripts

Europe PMC Funders Author Manuscripts

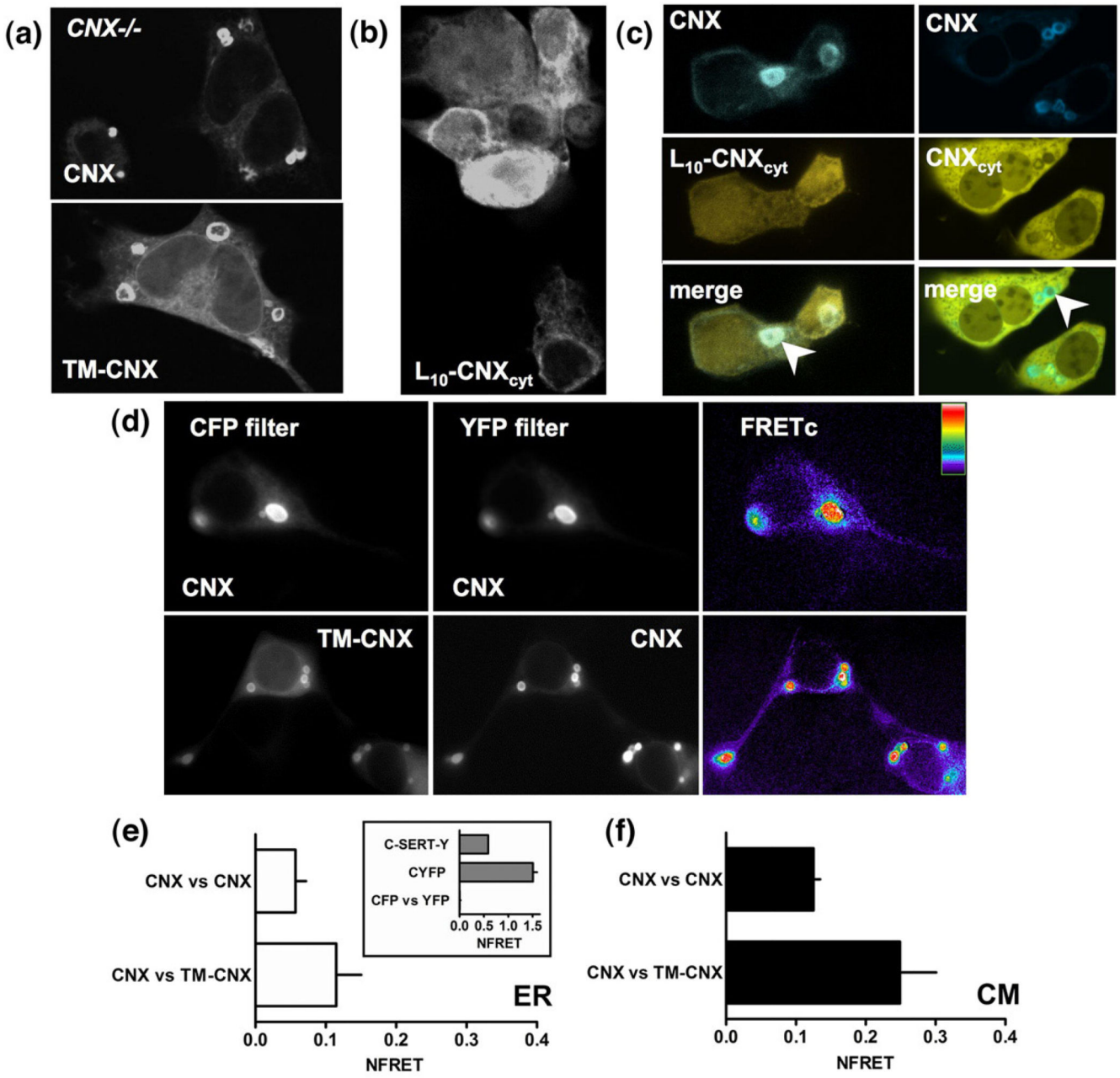

Fig. 3.

The transmembrane portion of calnexin supports targeting to concentric bodies. (a) YFP-tagged calnexin or a truncated form of calnexin lacking the luminal domain (TM-CNX) was visualized using confocal microscopy in transfected cnx−/− MEFs. (b) Confocal images of L10-calnexin-cyt (L_{10}-CNX_{cyt}) construct confirm that it associates with the intracellular membranes. (c) Co-expression of full-length calnexin with the L_{10}-$calnexin_{cyt}$ shows that the concentric membranes stained by calnexin contain L_{10}-$calnexin_{cyt}$, but there is no enrichment of the latter (left panel, arrowhead); co-expression of the YFP-tagged soluble C-terminus of calnexin (CNX_{cyt}) with the CFP-tagged calnexin shows that the soluble fragment is excluded from the concentric bodies (right, arrowhead). (d) FRET microscopy

and analysis was performed in transfected HEK293 cells as described under Materials and Methods; here, images constructed using only FRETc values are shown. Determination of NFRET was performed in ROIs within (e) the diffuse ER (n=10–15), and (f) multilamellar structures (n=36–89).

Europe PMC Funders Author Manuscripts

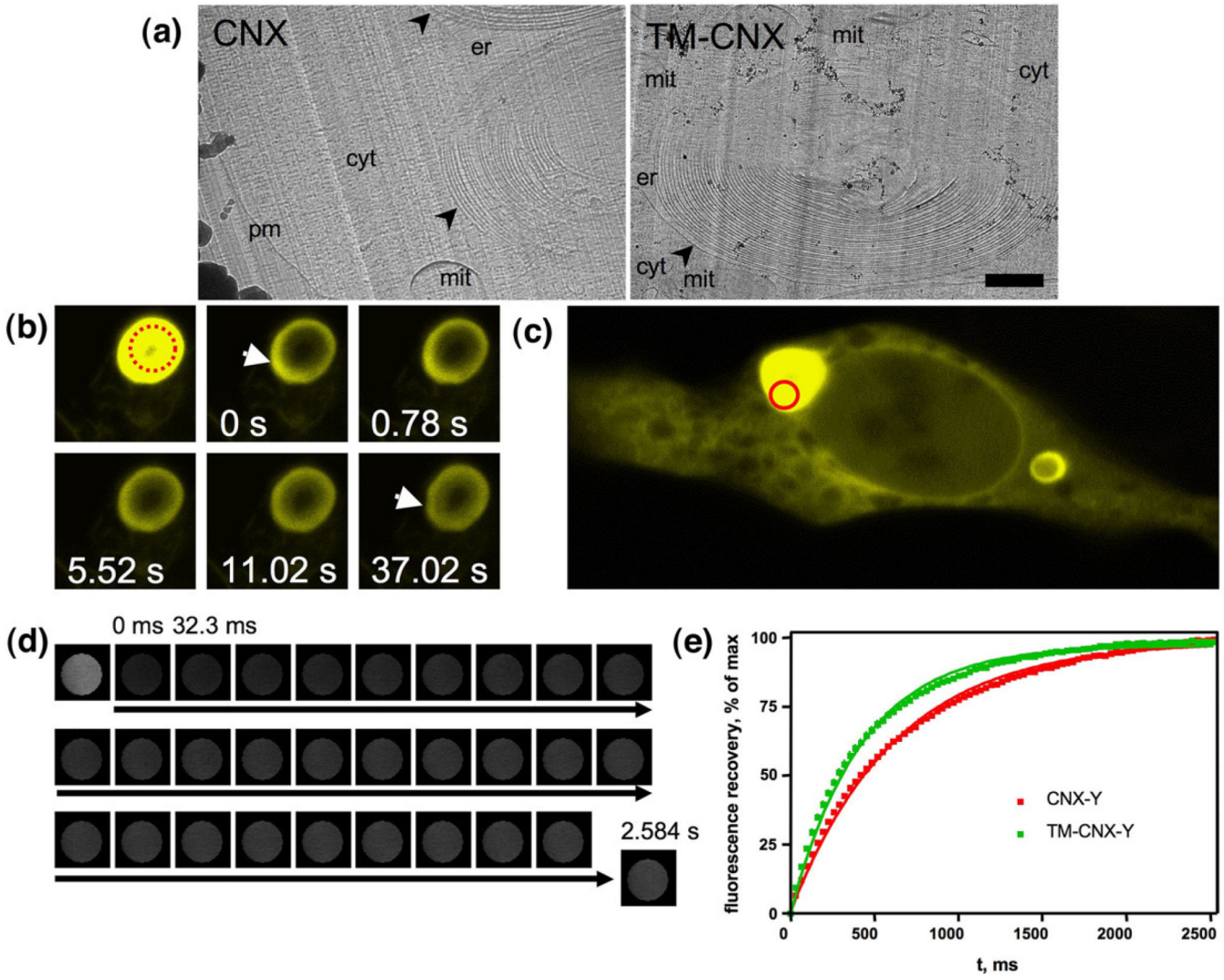

Fig. 4.

Calnexin constructs retain mobility in the multilamellar bodies. (a) CEMOVIS analysis confirms the multilamellar nature of the structures that form in the presence of calnexin or TM-calnexin ectopically expressed in HEK293 cells. Sample preparation and electron microscopy was performed as described in detail under Materials and Methods. Multilamellar bodies are indicated by arrowheads and labelled: er, ER lumen; cyt, cytosol; mit, mitochondrion; pm, plasma membrane. The scale bar represents 1 μm. (b) A concentric membrane body with CNX-YFP was photobleached, after which fluorescence recovery was monitored at indicated time points. Fluorescence is unevenly distributed in the region marked by an arrow at 0 s, compared to the rest of the membranous structure; after 11 s the fluorescent material was approximately homogenously distributed over the whorl membranes. (c) For more detailed analysis of CNX mobility within the multilamellar membranes, ROIs were selected photobleached as indicated by a circle. (d) Images of the photobleached area were saved as stacks; the small area of the ROI (d=1 μm) allowed for millisecond resolution of imaging. The resulting stacks were analysed using ImageJ as

described under Materials and Methods. (e) FRAP curves for YFP-tagged full-length calnexin (*n*=18) and TM-calnexin (*n*=14) derived from data such as those shown in (d). Recovery was defined as percentage of the maximum observed recovery; the absolute extent of recovery did not differ in wild-type and TM-CNX. Errors (SEM) are smaller than the symbol size and are therefore not seen.

Europe PMC Funders Author Manuscripts

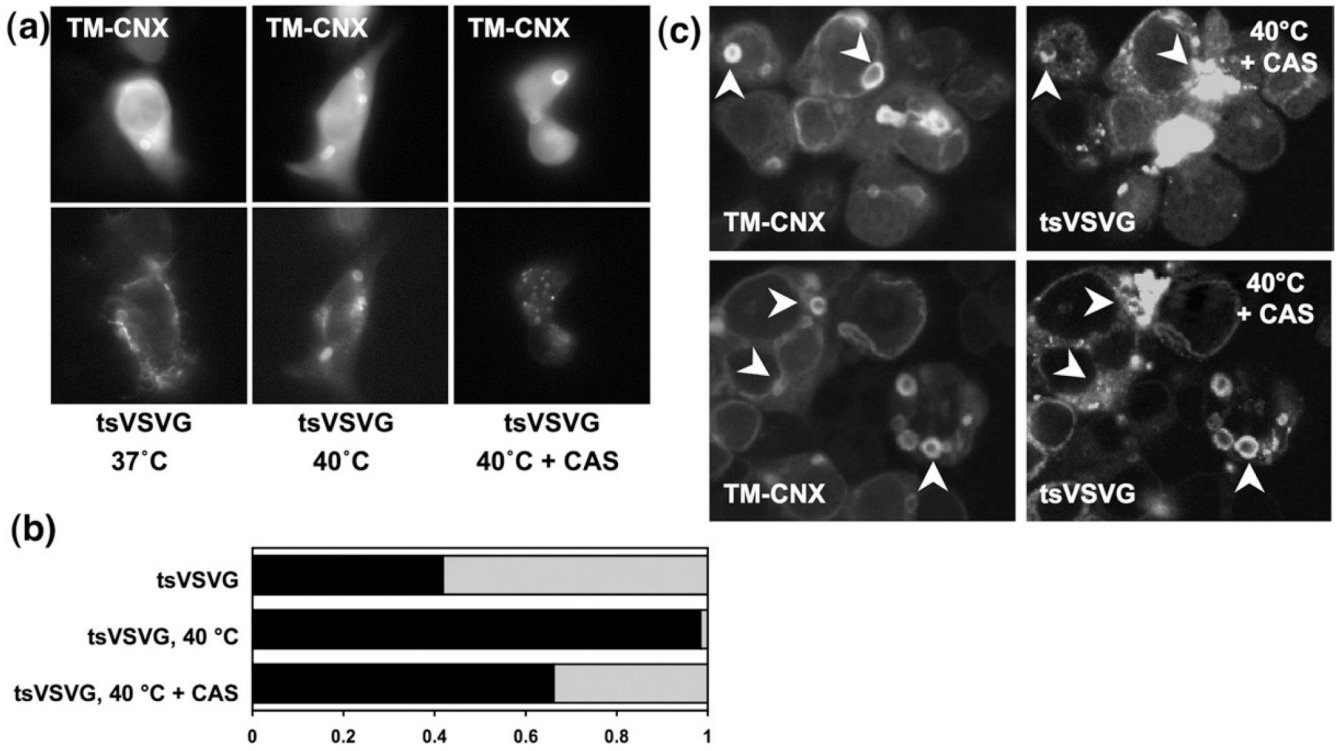

Fig. 5.

Calnexin retains its chaperone function within the concentric bodies. (a) The temperature-sensitive mutant of VSVG was co-expressed with TM-calnexin (TM-CNX); tsVSVG did not colocalize with TM-calnexin if cells were cultured at 37 °C (left). After 4 h at 40 °C, VSVG colocalized with TM-calnexin in all observed concentric bodies (middle). Four-hour pretreatment of cells with 1 mM castanospermine (CAS) reduced the number of concentric membrane bodies in which TM-calnexin and tsVSVG colocalized. (b) Quantification of tsVSVG in concentric bodies: the fraction thereof in which tsVSVG and TM-calnexin were colocalized is indicated by the filled area of the bar (tsVSVG, *n*=43; tsVSVG at 40 °C, *n*=128; tsVSVG at 40 °C+CAS, *n*=71). (c) Confocal microscopy reveals release of tsVSVG from multilamellar bodies and its clustering within, near or around the TM-calnexin-labelled regions of the multilamellar bodies. Arrowheads indicate the select multilamellar bodies and adjacent tsVSVG clusters.

Europe PMC Funders Author Manuscripts

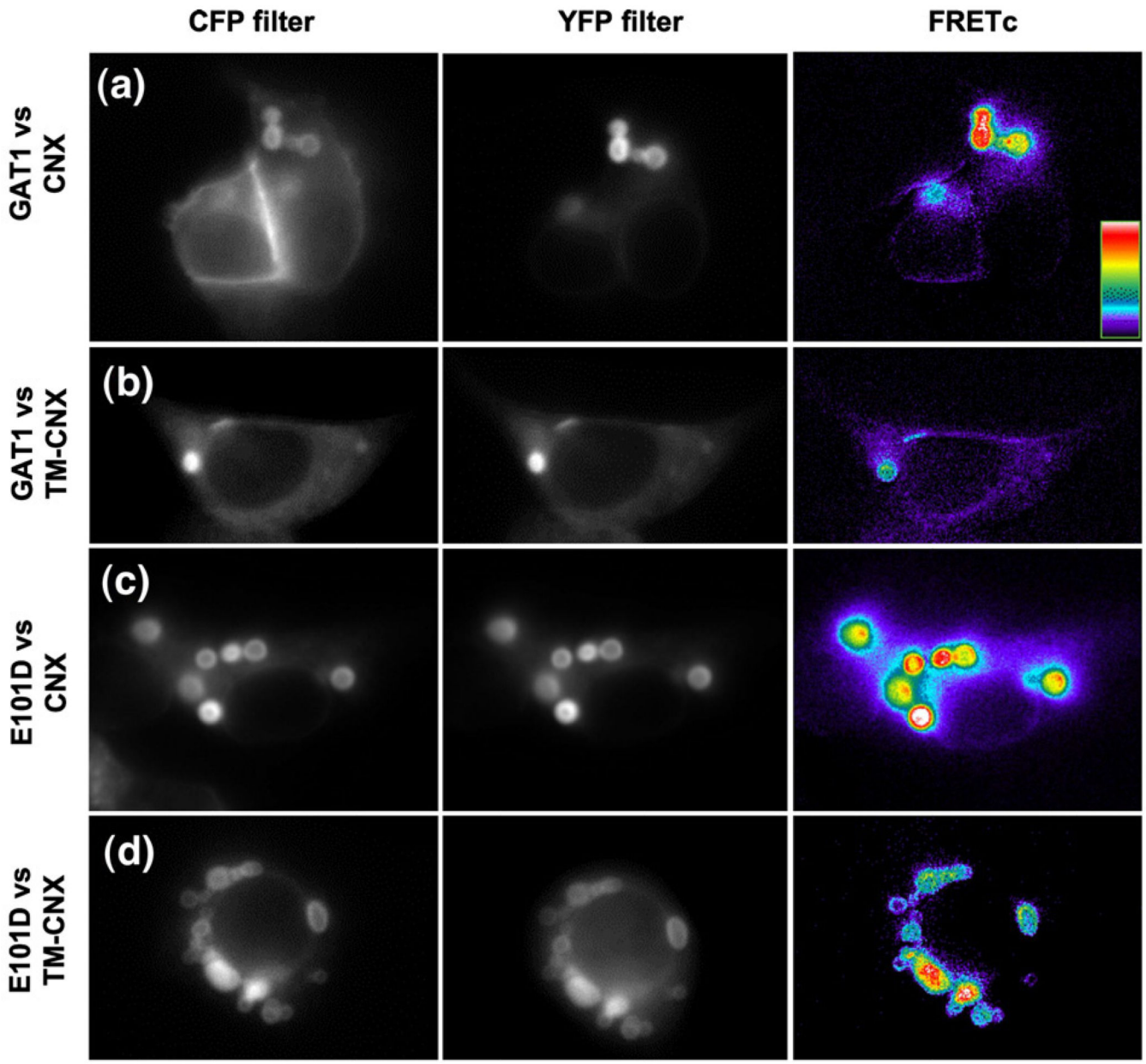

Fig. 6.

GAT1 and E101D colocalize with calnexin and TM-calnexin in concentric bodies. (a–d) HEK293 cells were co-transfected with plasmids driving the expression of CFP-tagged GAT1 (a, b) or of CFP-tagged GAT1-E101D (c, d) and of YFP-tagged calnexin or of YFP-tagged TM-calnexin, as indicated. Proteins were visualized by epifluorescence microscopy as outlined under Materials and Methods. The right-hand panels in each row represent FRETc images (computed as in Fig. 3 according to the equation in Materials and Methods); results for each pair of interacting proteins are summarized in Fig. 8.

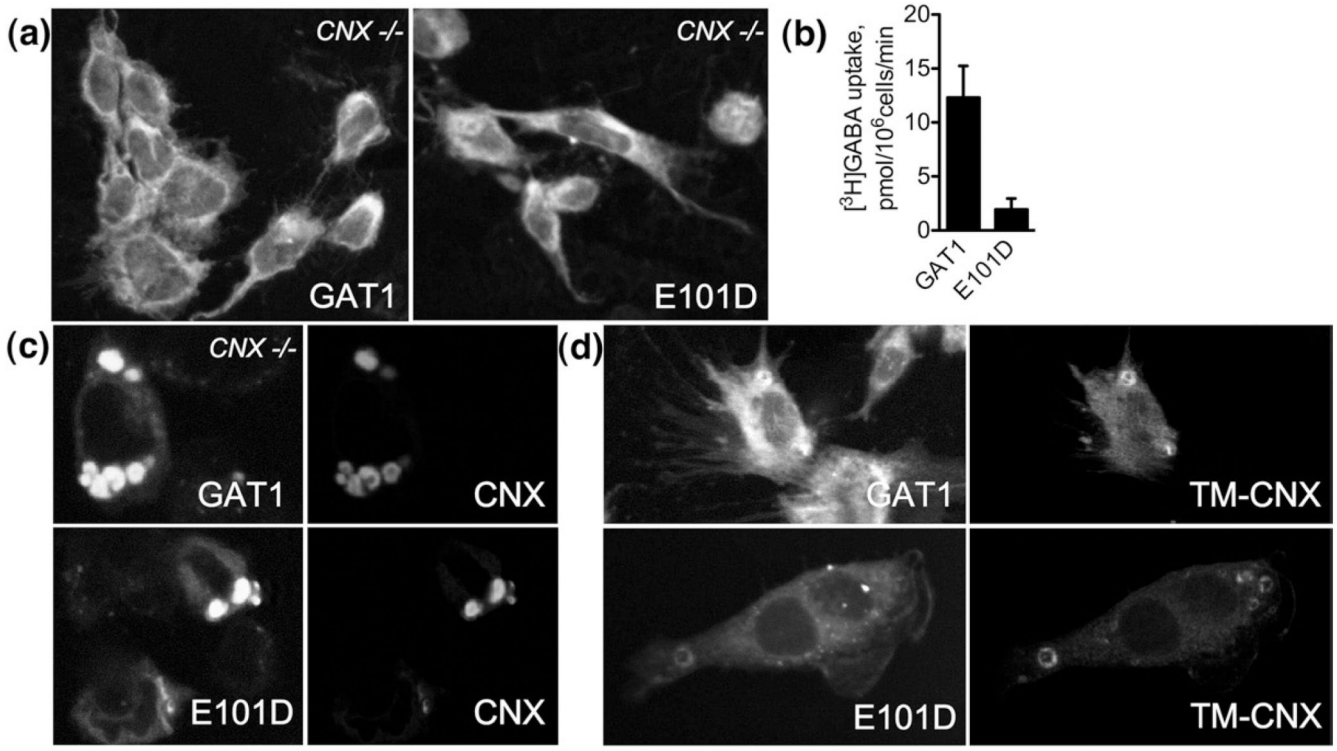

Fig. 7.

GAT1 molecules colocalize with calnexin-derived constructs in concentric membranes in the absence of endogenous calnexin. (a) Confocal microscopy images reveal poor cell surface expression of GAT1 and E101D. cnx−/− MEFs grown on glass coverslips were transfected with the indicated constructs and subjected to confocal microscopy analysis 48 h later. The bulk of the protein is retained inside the cell. (b) Whole-cell [^{3}H]GABA uptake experiments confirm lack of cell surface-expressed GAT1 and E101D. The experiments were performed as described in the legend to Fig. 1 and in Materials and Methods (the bars represent means±SEM from four experiments). (c and d) Confocal images show that GAT1 and E101D are enriched in the concentric membranes upon co-expression of calnexin or TM-calnexin.

Europe PMC Funders Author Manuscripts

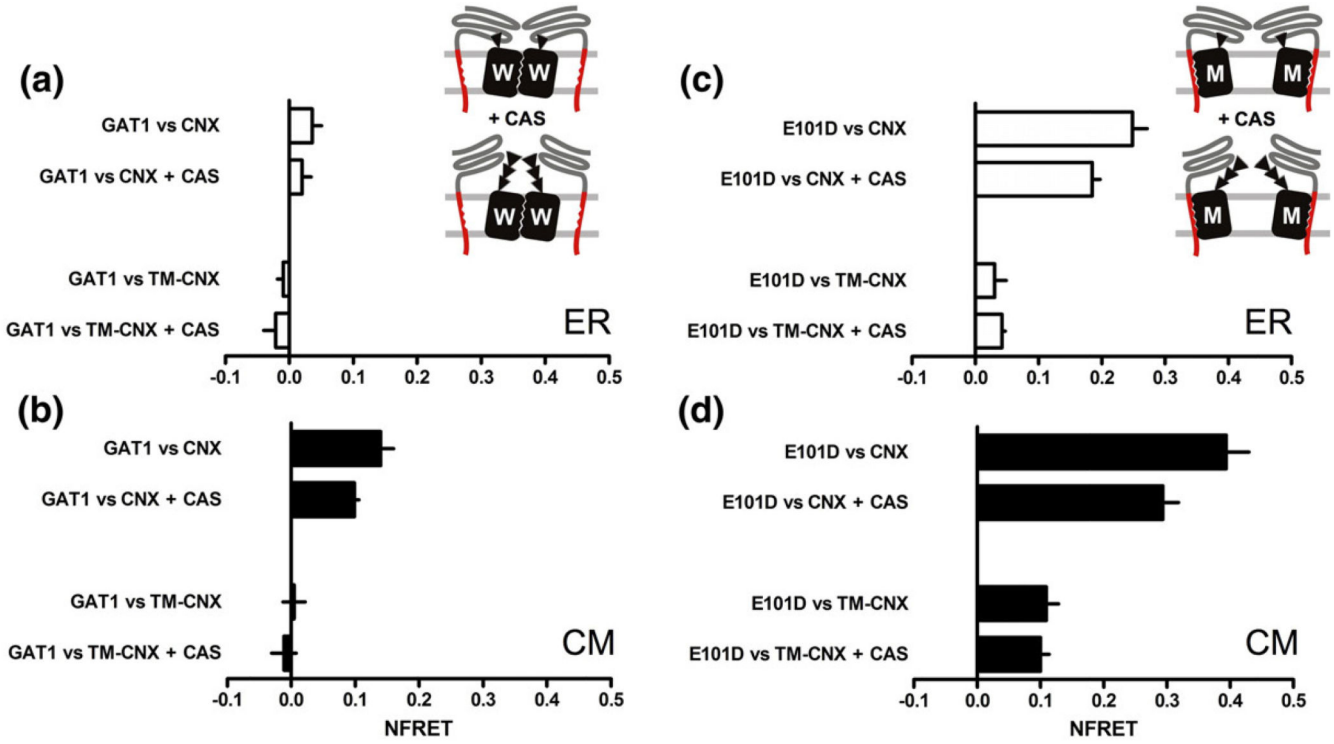

Fig. 8.

FRET analysis of co-expressed transporter/chaperone pairs. (a–d) HEK293 cells were co-transfected with the indicated plasmids. Images were captured by the three-filter method and the analysis was performed as described in the legend for Fig. 3d–f and under Materials and Methods to calculate the NFRET. Data represent means±SEM from two to five experiments; the numbers below correspond to numbers of experiments for each bar, from top down, in the indicated panels of Fig. 6: (a and b) 5, 5, 4, 3; (c and d) 3, 2, 4, 3. Each experiment included 18 separate determinations per FRET pair. The sketch for (a) and (b) illustrates the interaction between wild-type GAT1 and calnexin (CNX); pretreatment with castanospermine (1 mM, CAS) abolished the interaction with the lectin domain of calnexin. The sketch for (c) and (d) shows that pretreatment with castanospermine (1 mM, CAS) did not prevent sustained glycan-independent interactions with calnexin, including those mediated by the intramembrane portions of the interacting proteins. Data sets obtained from images of ROIs in the diffuse ER (indicated “ER” in a and c) and from ROI in the concentric membrane structures (indicated “CM” in b and d).

Europe PMC Funders Author Manuscripts

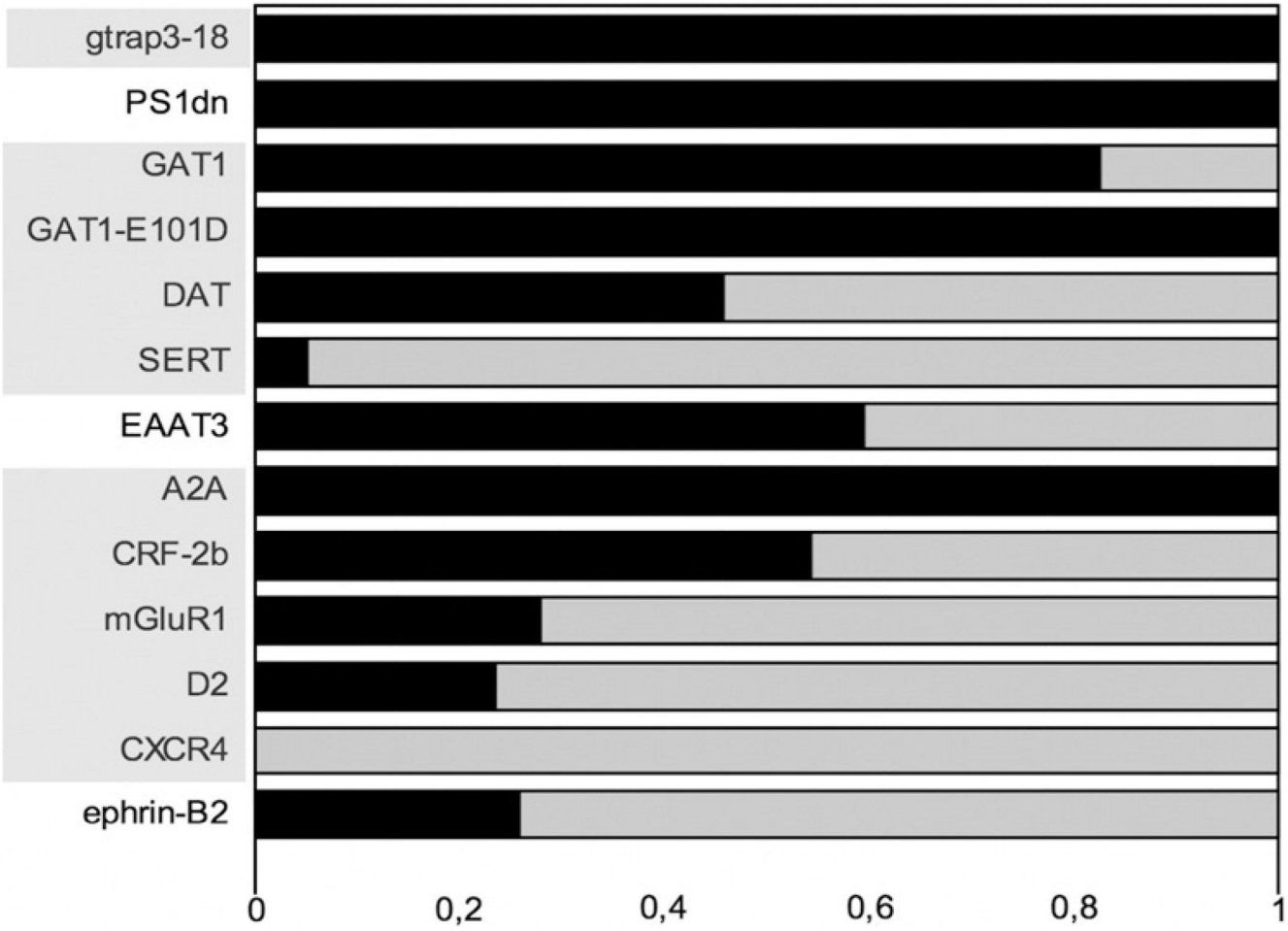

Fig. 9.

Quantification of selective targeting of membrane proteins to concentric bodies. The indicated proteins, tagged with a fluorescent protein, were co-expressed by transient transfection together with either CFP- or YFP-tagged TM-calnexin (as appropriate for dual-wavelength imaging/colocalization experiments) in HEK293 cells. Twenty-four hours later, coverslips with the transfected cells were mounted on an epifluorescence microscope stage and images of CFP and YFP/GFP channel were acquired. Only cells that co-expressed the protein of interest with TM-calnexin construct were analysed. The dark area of the bar indicates the fraction of concentric bodies that were positive for both TM-calnexin and the membrane protein of interest. The light field corresponds to that fraction of concentric bodies containing only TM-calnexin. The abbreviations of the proteins are shaded to indicate separate protein families (NSS, GPCRs, etc.). The *n* of observed concentric bodies for each co-expressed protein are as follows: GTRAP3-18, 27; PS1-dn, 19; GAT1, 58; GAT1-E101D, 47; DAT, 59; SERT, 58; EAAT3 (excitatory amino acid transporter-3), 37; A2A (A_{2A} adenosine receptor), 66; CRF-2b (corticotropin-releasing factor receptor-2b), 114; mGluR1 (metabotropic glutamate receptor-1), 75; D2 (D_2 dopamine receptor), 38; CXCR4 (CXC-chemokine receptor-4), 23; ephrin-B2, 146.

Europe PMC Funders Author Manuscripts

Table 1

FRAP analysis of co-expressed calnexin and GAT1 constructs

Co-expressed constructs, CFP- *versus* YFP-tagged	**$t_{1/2}$ (ms)**
Calnexin *versus* GAT1	
Calnexin	432.8±58.3
GAT1	379.1±31.5
Calnexin *versus* E101D	
Calnexin	426.8±64.2
E101D	442.9±67.5
TM-calnexin *versus* GAT1	
TM-calnexin	321.0±16.7
GAT1	387.3±25.8
TM-calnexin *versus* E101D	
TM-calnexin	320.3±25.8
E101D	365.2±44.7

Values shown are mean±SD, calculated as described under Materials and Methods.